

Are radio-loud active galactic nuclei really follow the same $M_{\text{BH}} - \sigma_*$ relation for normal galaxies?

Yi Liu^{1,2*} and Dong Rong Jiang¹

¹ Shanghai Astronomical Observatory, CAS, Shanghai 200030, China

² Graduate School of the Chinese Academy of Sciences, BeiJing 100039, China

Received month day; accepted month day

Abstract In order to examine the relationship between the black hole mass M_{BH} and stellar velocity dispersion σ_* in radio-loud active galactic nuclei (AGNs), we study two effects which may cause the uncertainty of black hole mass estimates for radio-loud AGNs: the relativistic beaming effect on the observed optical continuum radiation and the orientation effect on broad emission line width. After correcting these two effects in black hole mass calculations, we re-examine the $M_{\text{BH}} - \sigma_{[\text{OIII}]}$ relation for a sample of radio-loud and radio-quiet AGNs compiled from the literatures, and find the $M_{\text{BH}} - \sigma_{[\text{OIII}]}$ relation in radio-loud AGNs still deviate from that in nearby normal galaxies and radio-quiet AGNs. We also find there is no significant correlation between radio jet power and narrow [OIII] line width, indicating no strong interaction between radio jet and narrow line region. The deviation from $M_{\text{BH}} - \sigma_*$ relation in radio-loud AGNs may be intrinsic, or the [OIII] line width is not a good indicator of σ_* for radio-loud AGNs.

Key words: black hole physics — galaxies: active — galaxies: nuclei — quasars: general.

1 INTRODUCTION

There is abundant evidence show that the evolution of black holes and that of their host galaxies appears to be closely coupled. Kormendy & Richstone (1995) and Magorrian et al. (1998) showed that the central black hole mass correlates with the bulge mass and luminosity. The stellar velocity dispersion σ_* in the galactic bulge is also related with

* E-mail: yliu@shao.ac.cn

the mass of the center black hole (the $M_{\text{BH}} - \sigma_*$ relation). Gebhardt et al (2000a) and Ferrarese & Merritt (2000) found that the correlation between M_{BH} and σ_* is strong, suggesting a link between the formation of the bulge and the black hole. After investigating 31 nearby inactive galaxies, Tremaine et al. (2002) presented a relation as:

$$M_{\text{BH}} = 10^{8.13} (\sigma_*/(200 \text{ km s}^{-1}))^{4.02} M_{\odot}. \quad (1)$$

However, the bulge stellar velocity dispersion σ_* in the QSO is generally difficult to measure directly. Nelson & Whittle (1995; 1996) made a comparison of bulge magnitudes, [OIII] line widths, and σ_* in Seyfert galaxies, and found a good agreement between σ_* and $\sigma_{[\text{OIII}]}$ ($\sigma_{[\text{OIII}]} = \text{FWHM}([\text{OIII}])/2.35$) in statistical sense. The above relationship for normal galaxies also holds for active galaxies (Gebhardt et al. 2000b; Ferrarese et al. 2001; Wang & Lu 2001; Boroson 2003; Shields et al. 2003). The $M_{\text{BH}} - \sigma_{[\text{OIII}]}$ relation for all their radio-quiet sample follow that derived from nearby normal galaxies. It provides us a method to calculate the mass of black holes differ from that in Kaspi et al. (2000), which derived from active galactic nucleus broad emission line width and continuum luminosity.

However, Bian & Zhao (2004) presented a distinct result that the relationship between the mass of black hole and velocity dispersion in narrow line Seyfert1s and radio-loud AGNs deviates from the relationship which in radio-quiet AGNs and nearby normal galaxies. They suggested that the deviation in radio-loud AGNs from the $M_{\text{BH}} - \sigma_*$ relation might be due to the measurements uncertainties of $\sigma_{[\text{OIII}]}$ or M_{BH} . Bonning et al. (2005) tested the use of [OIII] line widths as a surrogate for σ_* by studying the $M_{\text{HOST}} - \sigma_{[\text{OIII}]}$ relation in a sample of quasars for which the host galaxies luminosity has been measured. They found an increase of $\sigma_{[\text{OIII}]}$ with σ_* in covering a wide range of measured or inferred σ_* , though the radio-loud AGNs have $\sigma_{[\text{OIII}]}$ smaller by 0.1 dex than radio-quiet QSOs of similar L_{HOST} . Greene & Ho (2005) compare σ_* with the widths of several narrow emission lines in a sample of narrow-line Seyfert galaxies from Sloan Digital Sky Survey (SDSS) and found that $\sigma_{[\text{OIII}]}$ exceeds σ_* about 0.13 dex. However, Salviander et al. (2006) found that $\sigma_{[\text{OIII}]}$ agrees with $\sigma_{[\text{OII}]}$ well in their sample of SDSS QSOs. Bian, Yuan & Zhao (2005) investigated the radial velocity difference between the narrow emission-line components of [OIII] in a sample of 150 SDSS NLS1 galaxies, and found that profile of [OIII] indicating two kinematically and physically distinct regions. The [OIII] line width depends not only on the bulge stellar gravitational potential, but also on the central black hole potential. Moreover, the interaction between the radio jets and the narrow line region (NLR), or radio jets inspire the star formation might also influence the physical and dynamical state of the [OIII] line width and its intensity.

Kaspi et al. (2000) derived an empirical relationship between the broad line region (BLR) size and the optical continuum luminosity at 5100\AA using the reverberation mapping technique. The empirical relationship has been frequently adopted to estimate the

BLR size and then to derive the black hole mass for AGNs samples. However, the relativistic jets of radio-loud AGNs both dominate the radio radiation and contribute significantly to the optical luminosity. The black hole mass in radio-loud AGNs would be overestimated by using the empirical relationship between the BLR size and optical luminosity at 5100\AA which is obtained from the sample of radio-quiet AGNs (Kaspi et al. 2000). On the other hand, as the jet axes are near to the line of sight for radio-loud AGNs, the geometrical effects might affect the observed widths of the broad $H\beta$ emission line and hence the black hole masses in radio-loud AGNs. These uncertainties in black hole mass calculation might influence the $M_{\text{BH}} - \sigma_{[\text{OIII}]}$ relation in radio-loud AGNs. In order to eliminating the beaming effect in optical continuum radiation for radio-loud AGNs, Wu et al. (2004) provided a method to calculate the black hole mass by a tight empirical relationship between the BLR size and the $H\beta$ emission line luminosity. In this paper, we re-compare the $M_{\text{BH}} - \sigma_{[\text{OIII}]}$ relation in a sample of radio-loud and radio-quiet AGNs after correcting the uncertainty for black hole mass, and then examine whether the $\sigma_{[\text{OIII}]}$ traces the σ_* in radio-loud AGNs. The relationship between the radio jet power and the [OIII] line width also be investigated. We used a cosmology with $H_0 = 70 \text{ km s}^{-1} \text{ Mpc}^{-1}$, $\Omega_M = 0.3$, $\Omega_\Lambda = 0.7$. All values of luminosity used in this paper are corrected to our adopted cosmological parameters.

2 SAMPLE AND METHOD

We started this work with the sample of Xu et al. (1999) which has 409 sources from the literature or through the NASA Extragalactic Database (NED). To estimate the black hole mass and $\sigma_{[\text{OIII}]}$, we then searched the literature for all available measurements of the full width of half maximum (FWHM) of both the broad $H\beta$ and narrow line $[\text{OIII}]_{5007}$, as well as of the line flux of $H\beta$. Finally, a sample of 123 AGNs was constructed, of which 25 are flat-spectrum radio-loud AGNs (FS), 35 are steep-spectrum (SS) radio-loud AGNs and 63 radio-quiet AGNs. The number of radio-loud AGNs in this sample is similar to that in Bian & Zhao (2004).

Table 1 lists our sample with the relevant information for each object. Columns (1)-(3) give the object's IAU name, radio spectrum type (FS denotes flat-spectrum and SS denotes steep-spectrum radio-loud AGNs, and RQ shows the radio-quiet AGNs respectively) and redshift. In columns (4)-(6), we list the black hole mass, the references for adopted FWHM of broad $H\beta$ emission line, and the references for adopted luminosity of broad line $H\beta$. In columns (7)-(8), we present the $\sigma_{[\text{OIII}]}$ and its references. A more detailed notation is given at the caption of Table 1.

Through the reverberation mapping method, Kaspi et al.(2000) presented an experiential relationship between the BLR size and the monochromatic luminosity at 5100\AA , and then the mass of the black holes can be estimated by using $M_{\text{BH}} = R_{\text{BLR}} V^2 G^{-1}$.

However, in radio-loud AGNs, there are two effects would cause the uncertainty of black hole mass estimate. Firstly, the radio observations shown that the orientation of the jets in the radio-loud AGNs, especially in the flat spectrum radio-loud AGNs, are close to the line of sight. The synchrotron emission of the jet are then Doppler boosted, and the contribution of the synchronization emission at the optical band may dominate over the thermal emission from the disk. So the mass of black hole in radio-loud AGNs could be overestimated. The second effect may cause the uncertainty of the black hole mass estimate is: if the geometry of the BLR is disk-like, the broad line width will depend on the orientation of the disk. The broad line widths of the radio-loud AGNs will be smaller than those in radio-quiet AGNs, even if they have similar black hole masses and BLR sizes (see Cao 2000; Xu & Cao 2006 for BL Lac objects). Wu et al. (2004) gave the relationship between the broad emission line $H\beta$ luminosity and size of broad line region which is derived from reverberation mapping method. Then the optical luminosity eliminated beaming effect can be calculated by using the broad line emission luminosity. As for the orientational effect for emission line width, Lacy et al. (2001) put forward using $R_c^{0.1}$ (R_c is the ratio of the core to the extended radio luminosity in the rest frame of the sources) factor to modify this effect, i.e for all radio-loud AGNs. However, this modification is invalid for the sources with $0 < R_c < 1$ and we only correct this orientation effect for the sources with $R_c > 1$. After these two corrections, we then calculated the mass of black hole in our sample and these compared the $M_{\text{BH}} - \sigma_{[\text{OIII}]}$ relation in radio-loud and radio-quiet AGNs. The results are plotted in Fig. 1.

3 RESULTS AND DISCUSSION

In Fig. 1(a)-(c) we plot the relationship between $\sigma_{[\text{OIII}]}$ and black hole mass M_{BH} from different methods, respectively. The black hole masses in Fig. 1(a) are estimated without any corrections. Fig. 1(b) shows the black hole mass with beaming effect correction but without orientation effect correction. In Fig. 1(c), the black hole masses are estimated with both beaming effect (for all radio-loud objects) and orientation effect (for only flat spectrum radio-loud AGNs) corrections. The solid circles denote flat spectrum radio-loud AGNs; the open circles present steep spectrum radio-loud AGNs, and the stars are for radio-quiet AGNs. The solid lines plotted in Fig. 1(a)-(c) show the $M_{\text{BH}} - \sigma_*$ relation defined by Tremaine et al. (2002).

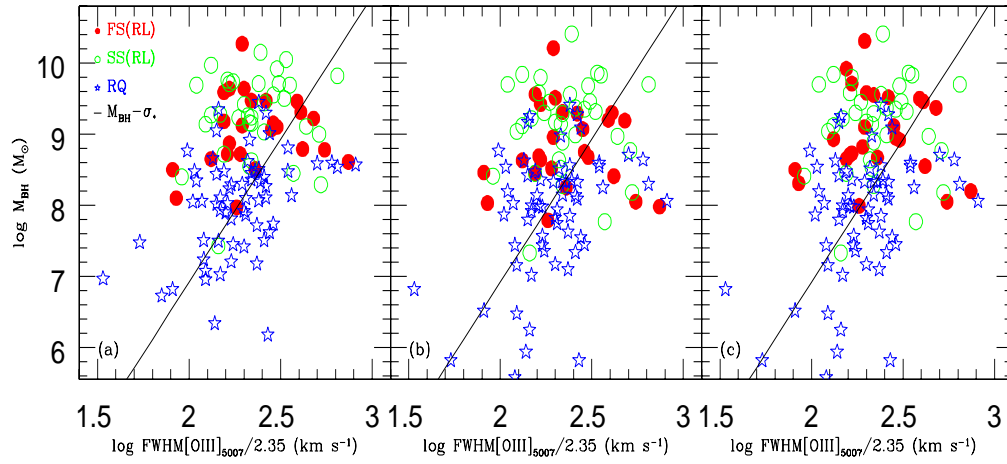


Fig. 1 Black hole mass versus σ_{OIII} for our sample. (a): Black hole mass derived from $H\beta$ line width without orientation correction and optical continuum luminosity. (b): Black hole mass derived from $H\beta$ line width without orientation correction and $H\beta$ luminosity. (c): Black hole mass estimated by correcting both the Doppler beaming effect and orientation effect. Solid circles denote the flat spectrum radio-loud AGNs; open circles show the steep spectrum radio-loud AGNs and pentagons plot the radio-quiet AGNs. The solid line shows $M_{\text{BH}} - \sigma_*$ relation from equation (1).

The beaming and orientation effects cause the black hole mass to move towards different opposite positions. On the one hand, similar as radio luminosity, the optical luminosity of radio-loud quasars can also be contaminated by the relativistically beamed jet emission. In fact, the optical emission of radio-loud quasars is a mixture of thermal and non-thermal emission, and tends to be orientated with their jets beamed along our line of sight, although not explicitly applicable on a source-by-source basis. Thus the black hole mass in radio-loud AGNs would be reduced after correcting the beaming effect for radio jet (Fig. 1(a) and Fig. 1(b)). On the other hand, if the geometry of the broad line region is disk-like, the object has smallest line width when the jet axis is along with the line of sight. After correcting for orientation effect, the black hole mass will be increased.

Figure 1(c) shows that the radio-quiet and radio-loud AGNs occupy two distinct regions in the $M_{\text{BH}}-\sigma_{[\text{OIII}]}$ plane. As the same results of other authors, the radio-quiet AGNs follow that relationship for our sample, but the radio-loud AGNs still deviate the $M_{\text{BH}}-\sigma_*$ relation of nearby normal galaxies, although the beaming effect and orientation effect in black hole mass calculation are eliminated. The black hole mass of radio-loud AGNs plotted in Fig. 1(c) are calculated by the width of $H\beta$ line and the luminosity of $H\beta$ which has been described in section 2. The beaming and orientation effect are two factors which will cause uncertainties of black hole mass. In order to eliminate the contamination by the emission from radio jets, continuum luminosity at 5100\AA was substituted by the broad line emission. However, the radio-loud AGNs remain the $M_{\text{BH}}-\sigma_*$ relation deviation after removing orientation factor. But we must keep in mind that the relationship between the broad line region radii R_{BLR} and broad emission line luminosity $L_{H\beta}$ which we used to calculate the black hole mass in our sample was derived from a sample for radio-quiet AGNs (Kaspi et al. 2000). Until now, the $R_{\text{BLR}} - L_{5100\text{\AA}}$ relation established from reverberation mapping method on radio-loud AGNs is still unavailable. Thus we are not clear whether the relationship between the R_{BLR} and $L_{5100\text{\AA}}$ or $L_{H\beta}$ for radio-loud AGNs is systematically different from that of radio-quiet AGNs. However, if this difference in radio-loud AGNs does exist, that means the R_{BLR} in radio-loud AGNs will one order of magnitude lower than that one in radio-quiet AGNs for the similar optical/line luminosity since the broad line width $\text{FWHM}_{H\beta}$ is similar for radio-loud and radio-quiet AGNs. However, the evidence for this kind of difference is not found so far, thus we think the uncertainties in black hole mass calculation might not be the main reason which leads this deviation in radio-loud AGNs.

Assuming radio-loud AGNs to follow the same $M_{\text{BH}}-\sigma_*$ relation defined by nearby normal galaxies and radio-quiet AGNs, we can derive the [OIII] line width which they should be from the $M_{\text{BH}}-\sigma_{[\text{OIII}]}$ relation and then derive the deviation to observed [OIII] line width ($\Delta[\text{OIII}]$). Figure 2 and Fig. 3 present the distribution of [OIII] line width and the distribution of $\Delta[\text{OIII}]$ for radio-loud and radio-quiet AGNs, respectively. The medians of [OIII] line width for these two sub-samples are similar (510 km s^{-1} for

radio-loud AGNs and 480 km s^{-1} for radio-quiet AGNs). However, it is obvious that the observed [OIII] line widths in radio-loud AGNs are smaller than those expected by the $M_{\text{BH}} - \sigma_*$ relation for normal galaxies.

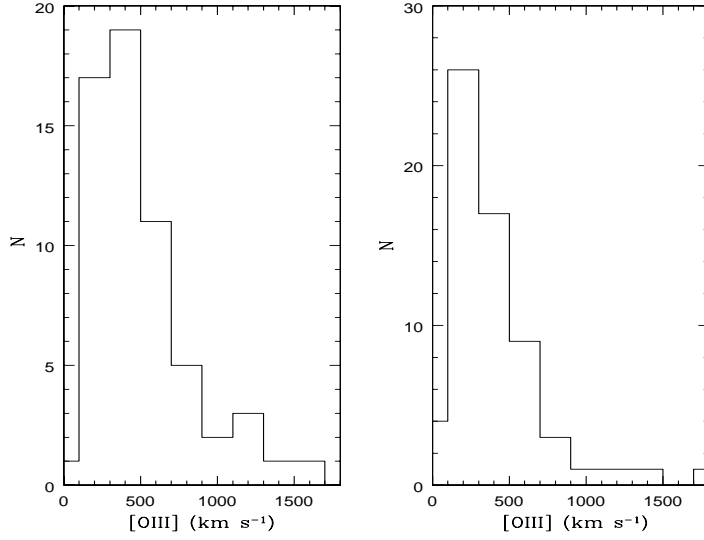


Fig. 2 Distribution of observed [OIII] line width for radio-loud AGNs (left) and radio-quiet AGNs (right).

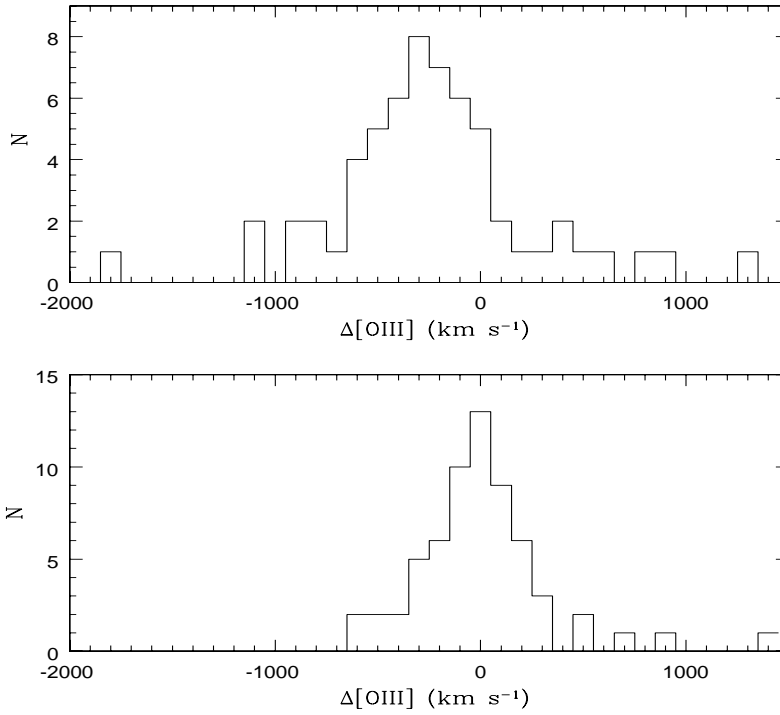


Fig. 3 Distribution of difference between the observed [OIII] line widths and expected by $M_{\text{BH}} - \sigma_*$ relation for radio-loud AGNs (upper) and radio-quiet AGNs (lower).

Although several groups investigated whether the $\sigma_{[\text{OIII}]}$ traces the σ_* , the use of $\sigma_{[\text{OIII}]}$ for σ_* is controversial. The outflow combined with extinction of the far side of the NLR might be as the result which caused asymmetry and non-Gaussian profile for [OIII] emission line (Nelson & Whittle 1995). Other strong iron emission lines, like FeII line, locates close to the [OIII] line may obscure them. There are some evidences suggesting that radio jets influence the physical and dynamical state of the NLR (de Bruyn & Wilson 1978; Ho & peng 2001). Nelson & Whittle (1996) found that the strong radio sources have broader [OIII] line width than weak radio sources. It seems that the jet plasma interacts with and accelerates the NLR, thus boosting the line width. However, radio-loud QSOs on average have smaller [OIII] line width than radio-quiet QSOs was found by Bonning et al. (2005). In the study for Smith et al. (1990), they found that no superviral [OIII] line widths among that objects with powerful radio jets at kpc scale.

The radio jet power, as a fundamental radio parameter indicating the energy transported through the radio jet from the central engine, can be used to investigate the relationship between the radio jet and the narrow line regions. We used the formula derived from Punsly (2005):

$$Q_{\text{jet}} = 5.7 \times 10^{44} (1+z)^{1+\alpha} Z^2 F_{151} \text{ erg s}^{-1} \quad (2)$$

$$Z \approx 3.31 - 3.65 \times [(1+z)^4 - 0.203(1+z)^3 + 0.749(1+z)^2 + 0.444(1+z) + 0.205]^{-0.125} \quad (3)$$

to estimate the jet power, where F_{151} is the optically thin flux density from the lobes measured at 151 MHz in units of Janskys, and the value of $\alpha \approx 1$ is suggested by the observations (Kellermann, PaulinyToth & Williams 1969) as a good fiducial value (see Punsly 2005 for more details). We also estimated the jet power by substituting the extrapolated extended 151 MHz flux density ($\alpha = 1.0$), instead of the measured 151 MHz flux since the 151 MHz emission can be from radio cores with Doppler boosted effects (Liu, Jiang & Gu. 2006). The relationship between the radio jet power and $\sigma_{[\text{OIII}]}$ is shown in Fig. 4, the solid circles denote all radio-loud AGNs in our sample, the open squares added on solid circles present objects with black hole mass in range from $10^{8.5} M_{\odot}$ to $10^{9.5} M_{\odot}$. Using the Spearman rank correlation analysis, we find a significant correlation between radio jet power and [OIII] line width with a correlation coefficient of $r = 0.32$ at $\gg 99$ per cent confidence. It should be noted with caution that this correlation may be caused by the common dependence of black hole mass. It may not be an intrinsic correlation, thus we check the correlation between the $\Delta[\text{OIII}]$ line width and radio jet power. Figure 5 shows the relationship between $\Delta[\text{OIII}]$ and radio jet power in our sample. However, no significant correlation is present between $\Delta[\text{OIII}]$ line width and radio jet power. It may support the scenario that there is no strong interaction between radio jet and narrow line region. Moreover, it should be cautious if there exists the interaction between the radio jet and narrow line region, this effect may broaden the narrow line width, and the

'true' [OIII] width will be narrower than that observed, which leads to enlarge the offset in $M_{\text{BH}} - \sigma_{[\text{OIII}]}$ for radio-loud AGNs. Greene & Ho (2005) found the presence of core radio emission seems to have no impact on the observed [OIII] line width, and we derive same result by using radio jet power. However, they found the extended radio sources appear to have narrower line width, as well as in our sample. In spite of the offset in the $M_{\text{BH}} - \sigma_{[\text{OIII}]}$ relation is unknown, Bonning et al. (2005) pointed out the radio-loud AGNs have $\sigma_{[\text{OIII}]}$ smaller by 0.1 dex than that of radio-quiet AGNs with similar L_{HOST} , the narrower $\sigma_{[\text{OIII}]}$ for radio-loud AGNs is the main reason to cause this offset. However, in our whole sample, we found the median of $\Delta[\text{OIII}]$ is about -300 km s^{-1} , that is about 0.2 dex in narrow line [OIII] width for radio-loud AGNs comparing to that one in nearby normal galaxies. If the radio-loud AGNs follow the $M_{\text{BH}} - \sigma_*$ relation in nearby normal galaxies, then the real σ_* in radio-loud AGNs should be more than 0.2 dex larger than that inferred from the [OIII] width.

Our sample is simply compiled from literatures, so selection effects may influence our results. If the deviation in $M_{\text{BH}} - \sigma_{[\text{OIII}]}$ for radio-loud AGNs was mainly caused by selection effects, which means that the radio-loud AGNs with low black hole masses and large narrow line [OIII] width might be lost. However, Laor (2000) studied the black hole mass in Palomar-Green quasar sample, and pointed out nearly all PG quasars with $M_{\text{BH}} > 10^9 M_{\odot}$ are radio-loud, while quasars with $M_{\text{BH}} < 3 \times 10^8 M_{\odot}$ are practically all radio-quiet. Therefore there is no this possibility that we have missing so much this kind of radio-loud AGNs with low black hole mass and large narrow line [OIII] width during our sample collecting, so we think the deviation may not mainly be caused by selection effects in our sample. And we need a complete matching sample including radio-loud and radio-quiet AGNs to get further study for the influence of selection effects.

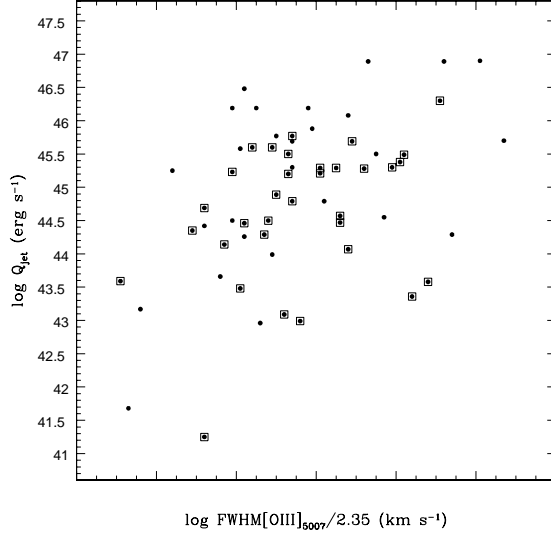


Fig. 4 The relationship between radio jet power and [OIII] line width for radio-loud AGNs. Solid circles denote all sample and squares added on solid circles denote black hole mass in range from $10^{8.5}M_{\odot}$ to $10^{9.5}M_{\odot}$.

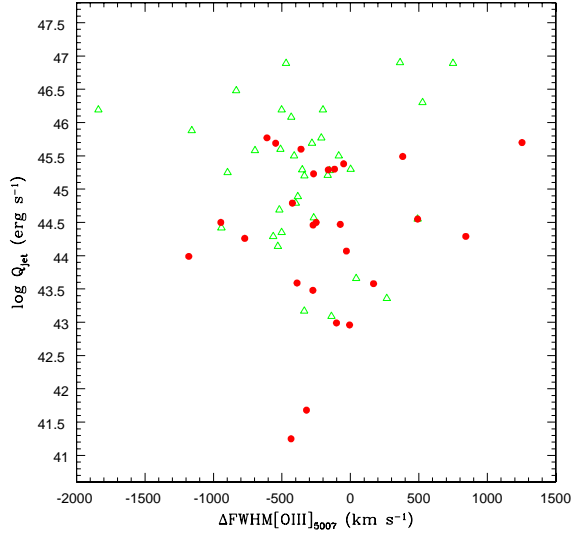


Fig. 5 The relationship between radio jet power and $\Delta\text{[OIII]}$ line width for radio-loud AGNs. Solid circles denote flat spectrum radio-loud AGNs and open triangles denote steep spectrum radio-loud AGNs.

The deviation from $M_{\text{BH}} - \sigma_*$ relation existing in radio-loud AGNs cannot be explained by beaming effect on optical continuum luminosity, orientation effect on broad line region and interaction between radio jet and narrow line region. The redshift of all objects in our sample are less than 1 because of adopting [OIII] and $H\beta$ emission line at the same time. It is worth investigating $M_{\text{BH}} - \sigma_{[\text{OIII}]}$ relation extends to higher redshift to avoiding the limitation in sample selection. One possible explanation is the [OIII] line might not be a good substitute for stellar velocity dispersion in radio-loud AGNs.

4 CONCLUSION

By estimating the black hole mass eliminating the beaming effects, we have re-investigated the relationship between black hole mass and narrow [OIII] line width for a sample of 60 radio-loud and 63 radio-quiet AGNs compiled from literature. Moreover, in order to know the influence from the radio emission to the narrow line region, the relationship between radio jet power and the narrow [OIII] width was also investigated. The main conclusions can be summarized as follows:

- After eliminating beaming effects in optical luminosity and correcting the orientation effect in broad line width, the $M_{\text{BH}} - \sigma_{[\text{OIII}]}$ relation in radio-loud AGNs still deviates from $M_{\text{BH}} - \sigma_*$ relation in nearby normal galaxies. However, it is confirmed again that the radio-quiet AGNs follow the $M_{\text{BH}} - \sigma_*$ relation in nearby normal galaxies.
- We find there is no significant correlation between the radio jet power and the narrow [OIII] line width, which indicating that the interaction between radio jet and narrow line region is not obvious. The deviation from $M_{\text{BH}} - \sigma_*$ in radio-loud AGNs cannot be explained by interaction in radio jet and narrow line region.
- The $M_{\text{BH}} - \sigma_{[\text{OIII}]}$ in radio-loud AGNs deviated from that relationship in nearby normal galaxies might not be caused by the uncertainty from black hole mass calculation, indicating that the narrow [OIII] line width might not be a good substitute for the stellar velocity dispersion. Another possible explanation is the radio-loud AGNs might not follow the same $M_{\text{BH}} - \sigma_*$ relation as normal galaxies and radio-quiet AGNs, and further investigation are needed.

Acknowledgements We are grateful to Xinwu Cao and Minfeng Gu for helpful discussions. We thank the anonymous referee for insightful comments and constructive suggestions. This work is supported by NSFC under grant 10373019 and 10333020. This research has made use of the NASA/ IPAC Extragalactic Database (NED), which is operated by the Jet Propulsion Laboratory, California Institute of Technology, under contract with the National Aeronautics and Space Administration.

References

- Appenzeller I., Wagner S. J. 1991, *A & A*, 250, 57 (AW91)
- Bian W., Zhao Y. 2004, *MNRAS*, 347, 607
- Bian W., Yuan Q. R., Zhao Y. H. 2005, *MNRAS*, 364, 187
- Bonning E. W., Shields G. A., Salviander S. et al. 2005, *ApJ*, 626, 89
- Boroson T. D., Green R. F. 1992, *ApJS*, 80, 109 (BG92)
- Boroson T. A. 2003, *ApJ*, 585, 647
- Brotherton M. S. 1996, *ApJS*, 102, 1 (B96)
- Cao X. W. 2004, *ApJ*, 609, 80
- Corbin M. R. 1991, *ApJ*, 371, 51 (C91)
- Corbin M. R., Boroson T. A. 1996, *ApJS*, 107, 69 (CB96)
- Dahari O., Michael M., Robertis D. 1988, *ApJS*, 67, 249 (D88)
- Delgado G. R. M., Heckman T., Leitherer C. et al. 1998, *ApJ*, 505, 174 (D98)
- de Bruyn A. G., Wilson A. S. 1978, *A&A*, 64, 433
- Feldman F. R., Weedman D. W., Balzano V. A. et al. 1982, *ApJ*, 256, 427 (F82)
- Ferrarese L., Merritt D. 2000, *ApJ*, 539, L9
- Ferrarese L., Pogge R. W., Peterson B. M. et al. 2001, *ApJ*, 555, L79
- Gebhardt K., Bender R., Bower G. et al. 2000a, *ApJ*, 539, L13
- Gebhardt K., Kormendy J., Ho L. C. et al. 2000b, *ApJ*, 543, L5
- Gelderman R., Whittle M. 1994, *ApJS*, 91, 491 (GW94)
- Gonzalez I. C., Carrasco L., Serrano A. et al. 1994, *ApJS*, 94, 47 (G94)
- Greene J. E., Ho, L. C. 2005, *ApJ* 627,721
- Grijp M. H. K., Keel W. C., Miley G. K. et al. 1992, *A & AS*, 96, 389 (G92)
- Grupe D., Beurermann K., Mannheim K. et al. 1999, *A & A*, 350, 805 (G99)
- Heckman T. M., Milee G. K., Green R. F. 1984, *ApJ*, 281, 525 (H84)
- Ho L. C., Peng C. Y. 2001, *ApJ*, 555, 650
- Jackson N., Browne W. A. 1991, *MNRAS*, 250, 414 (JB91a)
- Jackson N., Browne W. A. 1991, *MNRAS*, 250, 422 (JB91b)
- Kaspi S., Smith P. S., Netzer H. et al. 2000, *ApJ*, 533, 631
- Kellermann K. I., Pauliny-Toth I. I. K., Williams P. J. S. 1969, *ApJ*, 157, 1
- Kormendy J., Richstone D. 1995, *ARA&A*, 33, 581
- Kormendy J., Gebhardt K. 2001, in *AIP Conf. Proc.* 586, 20th Texas Symp. on Relativistic Astrophysics, ed. H. Martel & J. C. Wheeler (New York: AIP), 363
- Lacy M., Laurent-Muehleisen S. A., Ridgway S. E. et al. 2001, *ApJ*, 551, L17
- Lawrence C. R., Zucker J. R., REanhead C. S. et al. 1996, *ApJS*, 107, 541 (L96)
- Leighly K. 1999, *ApJS*, 125, 317 (L99)
- Liu Y., Jiang D. R., Gu M. F. 2006, *ApJ*, 637, 669
- Magorrian J., Tremaine S., Richstone D. et al. 1998, *AJ*, 115, 2285
- Marziani P., Sulentic J. W., Dultzin-Hacyan D. et al. 1996, *ApJS*, 104, 37 (M96)
- Mclure R. J., Dunlop J. S. *MNRAS*, 327, 199 (MD01)
- Miller P., Rawlings S., Saunders R. et al. 1992, *MNRAS*, 254, 93 (M92)
- Murayama T., Taniguchi Y. 1998, *AJ*, 115, 460 (MT98)
- Nelson C. H., Whittle M. 1995, *ApJS*, 99, 67
- Nelson C. H., Whittle M. 1996, *ApJ*, 465, 96
- Nerzer H. N., Brotherton M. S., Wills B. J. et al. 1995, *ApJ*, 448, 27 (N95)
- Oke J. B., Shields G. A., Korycansky D. G. 1984, *ApJ*, 277, 640 (O84)
- Osterbrock D. E., Koski A. T., Phillips M. M. 1976, *ApJ*, 206, 898 (O76)
- Osterbrock D. E., Shuder J. M. 1982, *ApJS*, 49, 1490 (OS82)
- Pererson B. M., Foltz C. B., Byard P. L. et al. 1982, *ApJS*, 49, 469 (P82)
- Peterson B. M., Foltz C. B., Crenshaw D. M. et al. 1984, *ApJ*, 279, 529 (P84)
- Punsly B. 2005, *ApJ*, 623, L9
- Robertis M. D. 1985, *ApJ*, 289, 67 (R85)

- Rosenblatt E. I., Malkan M. A., Sargent W. W. et al. 1994, ApJS, 93, 73 (R93)
- Salviander S., Shields G. A., Gebhardt K., et al. astro-ph/0601675
- Sergeev S. G., Pronik V. I., Sergeeva E. A. et al. 1999, AJ, 118, 2658 (S99)
- Shields G. A., Gebhardt K., Salviander S. et al. 2003, ApJ, 583, 124
- Simpson C., Ward M., Clements D. L. et al. 1996, MNRAS, 281, 509 (S96)
- Smith E. P., Heckman T. M., Illingworth G. D. 1990, ApJ, 356, 399
- Steiner J. E. 1981, ApJ, 250, 469 (S81)
- Stephens S. A. 1989, AJ, 97, 10 (S89a)
- Stickel M., Kuhr H., Fried J. W. 1993, A & AS, 97, 483 (S93)
- Stirpe G. M. 1990, A & AS, 85, 1049 (S90)
- Stockton A., Mackenty J. W., 1987, ApJ, 316, 584 (SM87)
- Sulentic J. W. 1989, ApJ, 343, 54 (S89b)
- Sulentic J. W., Marziani P., Zwitter T. et al. 2000, ApJ, 545, 15 (S00)
- Tadhunter C. N., Morganti R., Alighieri S. S. et al. 1993, MNRAS, 263, 999 (T93)
- Tran H. D. 1995, ApJ, 440, 565 (T95)
- Tremaine S., Gebhardt K., Bender R. et al. 2002, ApJ, 574, 740
- Wandel A., Peterson B. M., Malkan M. A. 1999, ApJ, 526, 579(W99)
- Whittle M. 1992, ApJS, 79, 49 (W92a)
- Wills B., Browne I. W. A. 1986, ApJ, 302, 56 (WB86)
- Wang T., Lu Y. 2001, A & A, 377, 52 (WL01)
- Winkler H. 1992, MNRAS, 257, 677 (W92b)
- Wu X. B., Wang R., Kong M. Z. et al. 2004 A & A, 424, 793
- Xu C., Livio M., Baum S. 1999, AJ, 118, 1169
- Xu Y., Cao, X. W. (accepted by ChJAA, 2006)

Table 1 M_{bh} and $\sigma_{[\text{OIII}]}$ for our sample. Col. (1): Object name. Col. (2): Type. Col. (3): Redshift. Col. (4): log of the black hole mass in units of solar mass. Col. (5): reference for FWHM of $\text{H}\beta$. (6): reference for $\text{H}\beta$ luminosity. Col. (7): log of the bulge velocity dispersion derived from FWHM of [OIII] line in units of erg s^{-1} . Col. (8): reference for FWHM of [OIII] line.

name	type	z	M_{BH}	Refs.	Refs.	$\sigma_{[\text{OIII}]}$	Refs.
(1)	(2)	(3)	(4)	(5)	(6)	(7)	(8)
0003+15	SS	0.450	9.22	BG92	S81	2.17	H84
0003+19	RQ	0.026	7.51	S99	S81	2.08	W92a
0007+10	FS	0.089	8.93	B96	S81	2.12	D88
0026+12	RQ	0.142	8.05	BG92	S81	2.02	D88
0046+31	RQ	0.015	8.48	T95	S81	2.19	W92a
0049+17	RQ	0.064	8.27	BG92	BG92	2.42	S89b
0050+12	RQ	0.061	8.54	M96	M96	2.81	M96
0052+25	RQ	0.155	7.72	BG92	SM87	2.37	S89b
0056-00	FS	0.717	8.55	B96	JB91a	2.62	B96
0109-38	RQ	0.012	7.50	MT98	MT98	2.16	MT98
0119+22	RQ	0.053	6.82	M92	M92	1.91	F82
0119-01	RQ	0.054	8.40	C91	S81	2.41	D88
0133+20	SS	0.425	9.83	JB91b	JB91a	2.55	CB96
0134+32	SS	0.367	8.77	B96	JB91a	2.71	B96
0159-11	FS	0.669	9.52	B96	O84	2.42	B96
0205+02	RQ	0.156	8.45	MD01	SM87	2.34	GW94
0211-01	RQ	0.028	7.81	S99	S99	2.23	D88
0232-09	RQ	0.043	8.66	W92b	W92b	2.13	W92a
0238+06	RQ	0.026	7.45	S90	S90	2.24	W92a
0316+41	FS	0.018	7.99	L96	L96	2.26	M96
0403-13	FS	0.571	9.10	M96	M96	2.29	N95
0405-12	SS	0.574	9.68	B96	M96	2.48	B96
0414-06	SS	0.781	10.41	B96	M96	2.39	B96
0418-55	RQ	0.004	7.24	W92b	W92b	2.08	W92a
0430+05	FS	0.034	8.31	S99	S99	1.93	H84
0434-10	RQ	0.035	7.62	P82	S81	2.44	W92a
0450-18	RQ	0.058	6.18	S89a	S89a	2.43	S89a
0513-00	RQ	0.033	8.62	P82	S99	2.32	W92a
0518+16	SS	0.759	8.18	JB91b	JB91b	2.72	GW94
0521-36	FS	0.055	8.05	S93	S93	2.74	S93
0538+49	SS	0.545	9.70	L96	GW94	2.81	L96
0551+46	RQ	0.021	7.74	OS82	S81	2.46	D88
0609+71	RQ	0.014	8.14	T95	S81	2.56	W92a
0645+74	RQ	0.020	8.10	S99	S81	2.31	W92a
0710+11	SS	0.768	10.87	B96	M96	2.25	B96

Table 1 Continued...

name	type	z	M_{BH}	Refs.	Refs.	$\sigma_{[\text{OIII}]}$	Refs.
(1)	(2)	(3)	(4)	(5)	(6)	(7)	(8)
0736+01	FS	0.191	8.67	B96	S81	2.36	B96
0738+31	FS	0.630	9.92	B96	S81	2.19	B96
0738+49	RQ	0.023	8.11	S99	S81	2.17	W92a
0742+31	FS	0.462	10.31	B96	M96	2.29	B96
0754+39	RQ	0.096	8.57	S89a	S89a	2.91	S89a
0837-12	SS	0.200	9.29	B96	S81	2.34	B96
0838+13	SS	0.684	8.45	B96	M96	2.19	B96
0903+16	SS	0.411	8.28	B96	JB91a	2.34	B96
0921+52	RQ	0.036	7.08	BG92	S81	2.09	W92a
0923+39	FS	0.699	9.55	B96	M96	2.34	B96
0945+07	SS	0.086	7.33	P84	O76	2.16	H84
0953+41	RQ	0.239	9.01	BG92	M96	2.44	M96
0955+32	SS	0.530	7.77	B96	M96	2.57	B96
1004+13	SS	0.240	9.17	B96	S81	2.30	B96
1007+41	SS	0.611	8.89	B96	M96	2.34	B96
1011-04	RQ	0.058	7.21	BG92	S96	2.23	WL01
1020+20	RQ	0.004	7.87	S99	S81	2.31	W92a
1022+51	RQ	0.045	6.97	BG92	S81	1.53	W92a
1028+31	FS	0.177	8.50	B96	JB91a	1.91	B96
1048-09	SS	0.344	9.04	BG92	SM87	2.09	H84
1049-00	RQ	0.357	9.45	BG92	SM87	2.38	M96
1100+77	SS	0.311	9.37	B96	SM87	2.41	B96
1103-00	SS	0.425	9.32	B96	SM87	2.52	B96
1116+21	RQ	0.177	8.59	BG92	M96	2.70	M96
1119+12	RQ	0.049	7.42	BG92	G99	2.30	F82
1133+21	RQ	0.030	6.96	WL01	G94	2.09	D88
1137+66	SS	0.646	9.56	B96	M96	2.38	B96
1150+49	FS	0.334	8.73	B96	SM87	2.22	B96
1156+29	FS	0.729	8.65	B96	B96	2.19	B96
1200+44	RQ	0.002	6.34	L99	S81	2.14	W92a
1202+28	RQ	0.165	8.92	BG92	M96	2.33	M96
1216+06	RQ	0.334	9.35	BG92	M96	2.16	M96
1217+02	FS	0.240	8.71	B96	JB91a	2.21	B96
1219+75	RQ	0.070	8.29	C91	S81	2.23	D88
1223+25	SS	0.268	9.45	JB91b	JB91a	2.27	H84
1226+02	FS	0.158	9.46	BG92	M96	2.61	M96
1229+20	RQ	0.064	8.06	BG92	S99	2.07	S89b
1237-05	RQ	0.009	8.35	P82	S99	2.04	W92a
1250+56	SS	0.320	8.52	B96	JB91a	2.33	B96

Table 1 Continued...

name	type	z	M_{BH}	Refs.	Refs.	$\sigma_{[\text{OIII}]}$	Refs.
(1)	(2)	(3)	(4)	(5)	(6)	(7)	(8)
1253-05	FS	0.536	8.20	WB86	M96	2.87	M96
1302-10	FS	0.286	8.92	BG92	M96	2.48	M96
1305+06	SS	0.599	9.35	B96	O84	2.46	B96
1307+08	RQ	0.155	8.30	BG92	SM87	2.29	AW91
1322-29	RQ	0.014	6.73	D98	D98	1.85	W92a
1346-30	RQ	0.016	8.07	W99	S81	2.38	S99
1351+64	RQ	0.087	8.81	BG92	M96	2.54	M96
1351+69	RQ	0.032	8.33	P82	S81	2.39	W92a
1352+18	RQ	0.158	8.60	BG92	S89a	2.78	S89a
1353+18	RQ	0.050	7.18	T95	T95	2.37	W92a
1354+19	FS	0.719	9.58	B96	B96	2.30	B96
1355-41	SS	0.313	9.58	AW91	T93	2.21	AW91
1411+44	RQ	0.089	8.11	BG92	M96	2.42	M96
1415+25	RQ	0.018	7.92	P82	M96	2.30	M96
1416-12	RQ	0.129	9.05	BG92	S00	2.15	AW91
1425+26	SS	0.366	9.84	B96	S81	2.12	B96
1434+59	RQ	0.031	8.02	OS82	S99	2.15	W92a
1439+53	RQ	0.037	7.90	T95	S81	2.20	W92a
1440+35	RQ	0.077	7.51	G99	S81	2.41	G99
1444+40	RQ	0.267	8.48	BG92	SM87	2.36	M96
1501+10	RQ	0.036	8.48	BG92	G92	2.03	D88
1510-08	FS	0.361	8.82	B96	S81	2.28	B96
1512+37	SS	0.371	9.70	B96	M96	2.04	B96
1522+15	FS	0.628	8.95	B96	B96	2.46	B96
1534+58	RQ	0.032	8.03	BG92	S81	2.21	W92a
1535+54	RQ	0.038	7.03	BG92	S81	2.17	W92a
1545+21	SS	0.264	9.14	B96	S81	2.33	B96
1612+26	RQ	0.131	8.24	BG92	S81	2.22	D88
1613+65	RQ	0.129	9.30	BG92	S90	2.42	D88
1617+17	RQ	0.114	8.77	BG92	BG92	1.99	D88
1618+17	SS	0.555	9.46	B96	M96	2.49	B96
1622+23	SS	0.927	9.80	OS82	S81	2.22	W92a
1626+55	RQ	0.133	8.48	BG92	R85	2.54	S89b
1641+39	FS	0.594	9.50	L96	JB91a	2.59	L96
1704+60	SS	0.371	9.30	B96	M96	2.24	B96
1828+48	SS	0.691	9.86	L96	JB91a	2.53	L96
1833+32	SS	0.058	8.64	C91	S81	2.32	H84
1845+79	SS	0.056	8.97	L96	S81	2.64	L96

Table 1 Continued...

name	type	z	M_{BH}	Refs.	Refs.	$\sigma_{[\text{OIII}]}$	Refs.
(1)	(2)	(3)	(4)	(5)	(6)	(7)	(8)
1928+73	FS	0.302	9.71	L96	M96	2.22	L96
1939-10	RQ	0.005	7.48	R93	W92b	1.73	W92a
2041-10	RQ	0.034	8.36	S99	M96	2.34	W92a
2130+09	RQ	0.063	7.93	BG92	S81	2.17	W92a
2135-14	SS	0.200	9.12	B96	M96	2.12	B96
2141+17	FS	0.213	9.37	JB91b	M96	2.68	M96
2201+31	FS	0.298	9.11	N95	M96	2.45	M96
2214+13	RQ	0.066	8.44	BG92	S81	2.15	W92a
2221-02	SS	0.056	8.41	WB86	S81	1.96	T93
2251+11	SS	0.323	8.99	BG92	M96	2.41	M96
2251-17	RQ	0.068	8.51	C91	S81	2.38	S89a

References: AW91: Appenzeller & Wagner (1991). B96: Brotherton (1996). BG92: Boroson & Green (1992). C91: Corbin (1991). CB96: Corbin & Boroson (1996). D88: Dahari et al. (1988). D98: Delgado et al. (1998). F82: Feldman et al. (1982). G92: Grijp et al. (1992). G94: Gonzalez et al. (1994). G99: Grupe et al. (1999). GW94: Gelderman & Whittle (1994). H84: Heckman et al. (1984). JB91a: Jackson & Browne (1991). JB91b: Jackson & Browne (1991). L96: Lawrence et al. L99: Leighly (1999). (1996). M92: Miller et al. (1992). M96: Marziani et al. (1996). MD01: Mclure & Dunlop (2001). MT98: Murayama & Taniguchi (1998). N95: Nerzer et al. (1995). O76: Osterbrock et al. (1976). O84: Oke et al. (1984). OS82: Osterbrock & Shuder (1982). P82: Peterson et al. (1982). P84: Peterson et al. (1984). R85: Robertis et al. (1985). R93: Rosenblatt et al. S81: Steiner (1981). (1993). S89a: Stephens (1989). S89b: Sulentic (1989). S90: Stirpe (1990). S96: Simpson et al. (1996). S99: Sergeev et al. (1999). S00: Sulentic et al. (2000). SM87: Stockton & Mackenty (1987). T93: Tadhunter et al. (1993). T95: Tran (1995). W92a: Whittle (1992). W92b: Winkler (1992). W99: Wandel et al. (1999). WB86: Wills & Browne (1986). WL01: Wang & Lu (2001).